doi:10.1093/brain/awaa063 BRAIN 2020: 143; 1114–1126 | 1114

BRAIN
A JOURNAL OF NEUROLOGY

Novel congenital disorder of O-linked glycosylation caused by GALNT2 loss of function

Monica Zilmer,[1,*] Andrew C. Edmondson,[2,3,*] Sumeet A. Khetarpal,[4,*] Viola Alesi,[5] Maha S. Zaki,[6] Kevin Rostasy,[7] Camilla G. Madsen,[8] Francesca R. Lepri,[5] Lorenzo Sinibaldi,[5] Raffaella Cusmai,[9] Antonio Novelli,[5] Mahmoud Y. Issa,[6] Christina D. Fenger,[10,11] Rami Abou Jamra,[12] Heiko Reutter,[13,14] Silvana Briuglia,[15] Emanuele Agolini,[5] Lars Hansen,[16] Ulla E. Petäjä-Repo,[17] John Hintze,[16] Kimiyo M. Raymond,[18] Kristen Liedtke,[18] Valentina Stanley,[19] Damir Musaev,[19] Joseph G. Gleeson,[19] Cecilia Vitali,[4] W. Timothy O'Brien,[20] Elena Gardella,[21] Guido Rubboli,[10,22] Daniel J. Rader,[2,3,4,*] Katrine T. Schjoldager[16,*] and Rikke S. Møller[10,23,*]

*These authors contributed equally to this work.

Congenital disorders of glycosylation are a growing group of rare genetic disorders caused by deficient protein and lipid glycosylation. Here, we report the clinical, biochemical, and molecular features of seven patients from four families with GALNT2-congenital disorder of glycosylation (GALNT2-CDG), an *O*-linked glycosylation disorder. *GALNT2* encodes the Golgi-localized polypeptide *N*-acetyl-D-galactosamine-transferase 2 isoenzyme. GALNT2 is widely expressed in most cell types and directs initiation of mucin-type protein *O*-glycosylation. All patients showed loss of *O*-glycosylation of apolipoprotein C-III, a non-redundant substrate for GALNT2. Patients with GALNT2-CDG generally exhibit a syndrome characterized by global developmental delay, intellectual disability with language deficit, autistic features, behavioural abnormalities, epilepsy, chronic insomnia, white matter changes on brain MRI, dysmorphic features, decreased stature, and decreased high density lipoprotein cholesterol levels. Rodent (mouse and rat) models of GALNT2-CDG recapitulated much of the human phenotype, including poor growth and neurodevelopmental abnormalities. In behavioural studies, GALNT2-CDG mice demonstrated cerebellar motor deficits, decreased sociability, and impaired sensory integration and processing. The multisystem nature of phenotypes in patients and rodent models of GALNT2-CDG suggest that there are multiple non-redundant protein substrates of GALNT2 in various tissues, including brain, which are critical to normal growth and development.

1 Department of Paediatrics, Danish Epilepsy Centre Filadelfia, 4293 Dianalund, Denmark
2 Department of Pediatrics, Division of Human Genetics, Section of Biochemical Genetics, Children's Hospital of Philadelphia, Philadelphia, PA 19104, USA
3 Department of Genetics, Perelman School of Medicine, University of Pennsylvania, Philadelphia, PA 19104, USA
4 Department of Medicine, Perelman School of Medicine, University of Pennsylvania, Philadelphia, PA 19104, USA
5 Medical Genetics Department, Bambino Gesù Children's Hospital, 00146 Rome, Italy
6 Clinical Genetics Department, Human Genetics and Genome Research Division, National Research Centre, Cairo 12311, Egypt
7 Department of Paediatric Neurology, Children's Hospital Datteln, Witten/Herdecke University, 45711 Datteln, Germany
8 Centre for Functional and Diagnostic Imaging and Research, Hvidovre Hospital, 2650 Hvidovre, Denmark
9 Neurology Unit, Department of Neuroscience, Bambino Gesù Children's Hospital, 00146 Rome, Italy
10 Department of Epilepsy Genetics and Personalized Medicine, Danish Epilepsy Centre Filadelfia, 4293 Dianalund, Denmark

Received August 27, 2019. Revised December 30, 2019. Accepted January 20, 2020. Advance access publication April 15, 2020

11 Amplexa Genetics A/S, 5000 Odense C, Denmark
12 Institute of Human Genetics, University of Leipzig, 04103 Leipzig, Germany
13 Department of Neonatology and Pediatric Intensive Care, University Hospital of Bonn, 53012 Bonn, Germany
14 Institute of Human Genetics, University Hospital of Bonn, 53012 Bonn, Germany
15 Medical Genetics of Messina University, 98125 Messina, Italy
16 Copenhagen Centre for Glycomics, Department of Cellular and Molecular Medicine, Faculty of Health Sciences, University of Copenhagen, 2200 Copenhagen N, Denmark
17 Research Unit of Biomedicine, University of Oulu, 90014 University of Oulu, Finland
18 Biochemical Genetics Laboratory, Department of Laboratory Medicine and Pathology, Mayo Clinic, Rochester, MN 55905, USA
19 Laboratory for Pediatric Brain Disease, Howard Hughes Medical Institute, Rady Children's Institute for Genomic Medicine, University of California, San Diego, CA 92093, USA
20 Institute for Translational Medicine and Therapeutics, University of Pennsylvania, Philadelphia, PA 19104, USA
21 Department of Neurophysiology, Danish Epilepsy Centre Filadelfia, 4293 Dianalund, Denmark
22 Institute of Clinical Medicine, University of Copenhagen, 2200 Copenhagen N, Denmark
23 Institute for Regional Health Services, University of Southern Denmark, 5000 Odense C, Denmark

Correspondence to: Dr Rikke S. Møller
Department of Epilepsy Genetics and Personalized Medicine
Danish Epilepsy Centre Filadelfia
Kolonivej 1, 4293 Dianalund, Denmark
E-mail: rimo@filadelfia.dk

Correspondence may also be addressed to: Dr Katrine T. Schjoldager
Copenhagen Centre for Glycomics
University of Copenhagen
Blegdamsvej 3, 2200 Copenhagen N, Denmark
E-mail: schjoldager@sund.ku.dk

Keywords: congenital disorders of glycosylation; *O*-glycosylation; GALNT2; apolipoprotein C-III glycosylation; HDL-cholesterol

Abbreviations: apoC-III = apolipoprotein C-III; CDG = congenital disorder of glycosylation; GalNAc = *N*-acetyl-D-galactosamine; GALNT = polypeptide *N*-acetylgalactosaminyl-transferase; HDL-C = high density lipoprotein cholesterol; WES = whole-exome sequencing

Introduction

Congenital disorders of glycosylation (CDG) are a heterogeneous group of rare genetic disorders with a wide range of phenotypes. They arise from defects in protein, lipid or proteoglycan glycosylation pathways (Jaeken and Peanne, 2017). Deficiencies in glycosyltransferase genes are found to cause more than half of the some 130 reported CDG (Ng and Freeze, 2018).

Recently, deficiencies in glycosyltransferase genes of larger isoenzyme families have been shown to cause CDG with less severe clinical phenotypes (Joshi *et al.*, 2018). Traditional biomarker assays, such as characterization of the *N*-glycosylation state of plasma transferrin (Wopereis *et al.*, 2007), do not generally identify these newer CDG (Ng and Freeze, 2018). Discovering and validating such CDG, as well as identifying the molecular mechanisms underlying deficiencies in glycosylation that affect only a few proteins, remain challenging endeavours.

Mucin-type or *N*-acetyl-D-galactosamine (GalNAc)-type *O*-glycosylation is initiated by a large family of polypeptide GalNAc-transferase (GALNT, also known as GalNAc-T) isoenzymes with considerable overlapping functions in directing *O*-glycosylation of proteins. The GALNTs represent an emerging gene family where aberrant function of a single isoenzyme can result in extremely subtle loss of non-redundant glycosylation of one or few proteins and lead to CDG (Joshi *et al.*, 2018). This was first realized with the discovery that pathogenic variants in *GALNT3* caused familial tumoral calcinosis (Topaz *et al.*, 2004). It was later demonstrated that pathogenesis of familial tumoral calcinosis is caused by highly specific loss of *O*-glycosylation at a single *O*-glycosite in phosphaturic factor fibroblast growth factor 23 (FGF23), which co-regulates biological activity and phosphate homeostasis (Kato *et al.*, 2006).

A second member of the *GALNT* family, *GALNT2*, was initially implicated in human lipoprotein metabolism by genome-wide association studies (GWAS) (Kathiresan *et al.*, 2008). Previously, we described two unrelated individuals with intellectual disability and biallelic variants in *GALNT2* who had reduced levels of high-density lipoprotein cholesterol (HDL-C) and plasma triglycerides (Khetarpal *et al.*, 2016). Unique protein substrates for the encoded GALNT2 included the lipoprotein lipase inhibitors angiopoietin-like 3 (ANGPTL3), apolipoprotein C-III (apoC-III) (Schjoldager *et al.*, 2012), and phospholipid transfer protein (PLTP) (Khetarpal *et al.*, 2016). Using these proteins as biomarkers,

we confirmed complete loss-of-function of GALNT2 in two unrelated individuals (Khetarpal *et al.*, 2016). One of the two patients (c.865C>T; p.Gln289*) was separately reported to have a complex medical history with very severe intellectual disability, seizures, autism spectrum disorder, aggressive behaviour, feeding problems in infancy, short stature, constipation, strabismus, and inguinal hernia (Reuter *et al.*, 2017). *GALNT2* was suggested as a novel candidate gene, potentially explaining the observed neurodevelopmental disorder.

Here, we report three additional families with six previously unpublished individuals exhibiting biallelic pathogenic variants in *GALNT2*. We comprehensively describe the clinical, biochemical, and molecular characteristics of a total of seven patients with GALNT2-CDG. In particular, we confirm the loss of plasma apoC-III *O*-glycosylation as a robust biomarker assay for the disorder. Furthermore, we demonstrate that the physical and behavioural characteristics of rodent models of GALNT2-CDG with knockout of *Galnt2* recapitulate many of the features seen in patients, including poor growth and neurodevelopmental and lipid abnormalities.

Patients and methods

This study was performed in accordance with ethical principles for medical research outlined in the Declaration of Helsinki. All relevant approvals from the institutional ethics committees of the participating institutions were obtained as well as written informed consent from all patients' guardians before inclusion in the study.

Patients

We describe seven patients (Patients A–G) with biallelic pathogenic *GALNT2* variants from four families (Families 1–4), including six previously unpublished patients. Patient A from Family 1 was previously published (Khetarpal *et al.*, 2016; Reuter *et al.*, 2017); the present study also included a younger affected brother (Patient B). Patients were recruited from research or diagnostic programs in Europe and the Arab Republic of Egypt. Grouping of clinical data for this series was facilitated by GeneMatcher (Sobreira *et al.*, 2015). All patients were clinically evaluated by neuropaediatricians and clinical geneticists at their respective tertiary healthcare centres. Patients underwent comprehensive history and physical examinations, fasting blood chemistry, genetic testing, EEG and brain MRI scan. EDTA plasma samples for western blot and mass spectrometry analysis were obtained by venepuncture, red cells were pelleted by centrifugation and plasma was separated, frozen and shipped on dry ice to the analysing laboratories. Various protocols were used to obtain brain MRI scans, which were of varying field strengths, slice thicknesses, and image qualities (3 T Dicom format to 6 mm slice thickness hard copy film photos at 1.5 T). The same neuroradiologist evaluated all scans. In some patients, hand X-ray, echocardiography, and abdominal ultrasonography were also performed.

Growth analysis

Patient growth was evaluated utilizing the growth charts indicated in Table 2 and in the Supplementary material. Short stature was defined as length/height <–2 standard deviations (SD) for sex and chronological age (Wit *et al.*, 2007; Quigley and Ranke, 2016). Microcephaly was defined as head circumference <3rd percentile for sex and chronological age as an approximation to head circumference <–2 SD (Ashwal *et al.*, 2009).

Molecular genetic analysis

Patient A from Family 1 was enrolled in a study for recessive heritable causes of intellectual disability (Abou Jamra *et al.*, 2011) and underwent research whole-exome sequencing (WES), as previously described (Khetarpal *et al.*, 2016). From the same family, Patient B underwent Sanger sequencing to confirm biallelic inheritance of the familial *GALNT2* variant identified in Patient A. Patient C from Family 2 had clinical single nucleotide polymorphism (SNP) array performed, which identified several regions of homozygosity. Genes in these regions were subsequently analysed by next-generation sequencing (NGS). Patient D from Family 3 underwent Sanger sequencing to confirm biallelic inheritance of the familial *GALNT2* variant identified in Patient E. Patient E, also from Family 3, underwent clinical WES using the NovaSeq 6000 System at the Danish Epilepsy Centre as part of the diagnostic work-up. Research WES was performed for both affected family members in Family 4 (Patients F and G). In this family, WES was performed by using Illumina HiSeq4000, which yields 150-bp paired-end reads covering 85% of the exome at 20× and >96% of the exome at >12×. The GATK best-practices pipeline was used to identify SNP and INDEL variants. Variants were prioritized by minor allele frequency (<0.1% in research exome database of >5000 individuals), conservation and predicted effect on protein function. Variants were confirmed by Sanger sequencing.

ApoC-III isoform analysis

Western blot analysis of plasma apoC-III was performed as previously described (Khetarpal *et al.*, 2016) with minor modifications (Supplementary material). Mass spectrometry analysis of apoC-III isoforms was performed at Mayo Clinic Laboratories (clinical test ID: CDG, Supplementary material).

Galnt2 knockout rodent models

Animal studies were approved by the Institutional Animal Care and Use Committees of the University of Pennsylvania (mice) and SAGE laboratories (rats). Rodents were generated, bred, and genotyped as previously described (Khetarpal *et al.*, 2016). Rodents were subject to alternating 12-h light/dark cycles and given access to standard chow diet *ad libitum*. Rodents were housed with age- and sex-matched littermate wild-type controls

at two to four animals per cage. Mouse behavioural testing (Supplementary material) was performed in female mice at 8–10 weeks of age. Investigators were blinded during scoring of behavioural assays.

Statistical analysis

Data represent means, with error bars showing ± SDs. Genotype distributions of rodent offspring were analysed by using the χ^2 test against expected Mendelian distribution. One-way ANOVA with Tukey's post-test was used to analyse rodent body weight. Two-tailed unpaired Student's *t*-test was used to analyse organ weights and data for open-field activities, acoustic startle habituation and prepulse inhibition trials. Two-way repeated measures ANOVA was used to analyse rotarod data (with trial number and genotype as factors), acoustic startle data (with dB and genotype as factors) and olfactory data (with odorant and genotype as factors). Two-way ANOVA with Tukey's post-test was used to analyse social choice data (with cue type and genotype as factors). Level of significance was set at $P \leqslant 0.05$.

Data availability

Data supporting the findings of this study are available from the corresponding author, upon reasonable request.

Results

Genetic changes in patients

Family pedigrees are shown in Fig. 1A. Family histories and *GALNT2* genetic changes are shown in Table 1.

Patients A and B (Family 1) were siblings born of consanguineous parents. Both were homozygous for a previously reported pathogenic variant (c.865C>T; p.Gln289*) in *GALNT2* (Khetarpal *et al.*, 2016).

In Patient C (Family 2), SNP array identified homozygous inheritance of 11.8 Mb and 2.6 Mb across the 1q41q42.2 and 2q37.3 chromosomal regions, respectively. The only potentially clinically significant homozygous variant identified through clinical NGS of genes in these regions of homozygosity was a homozygous pathogenic variant (c.598C>T; p.Arg200*) in *GALNT2*. As anticipated, the parents were both confirmed heterozygous for this variant. There was no known parental consanguinity, but the grandfathers were from the same small village. The variant was reported in gnomAD in one heterozygous individual with reference SNP ID rs1431963909.

Patients D and E (Family 3) were siblings who were both homozygous for a novel pathogenic variant (c.296dup;

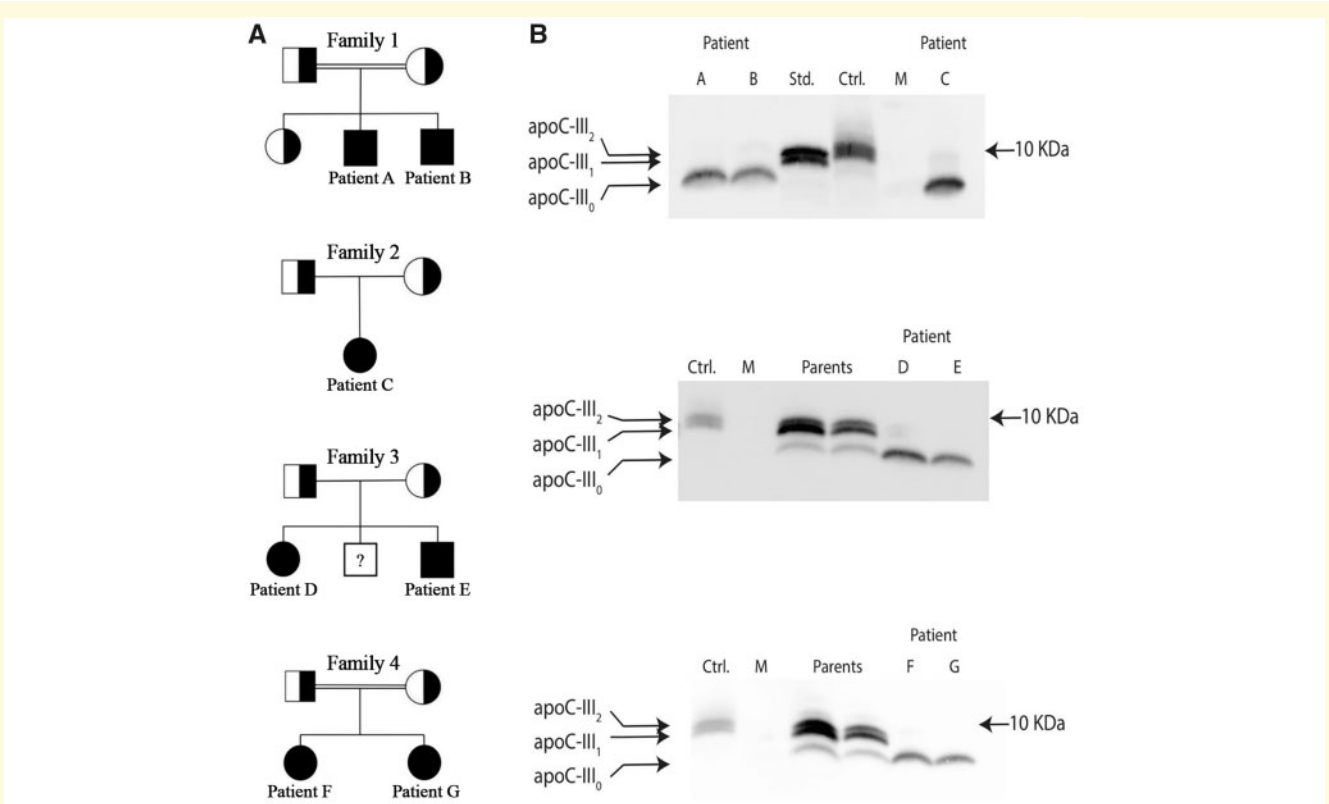

Figure 1 Family pedigrees of GALNT2-CDG patients and immunoblots of plasma apoC-III. (**A**) Family pedigrees of GALNT2-CDG patients. (**B**) Immunoblots of plasma apoC-III for probands and family controls of the *GALNT2* loss-of-function mutation. Migration positions of three major apoC-III isoforms: non-glycosylated apoC-III (apoC-III$_0$) lacking any *O*-glycan modification; monosialylated apoC-III (apoC-III$_1$) containing *N*-acetylgalactosamine, galactose, and one terminal sialic acid; and disialylated apoC-III (apoC-III$_2$) containing *N*-acetylgalactosamine, galactose, and two terminal sialic acids, are indicated on the left. Ctrl = analysis with healthy control plasma; M = marker lane with protein standard; Std = analysis with standard human apoC-III purified from plasma.

Table 1 Family history, *GALNT2* genetic changes and apoC-III glycosylation changes in GALNT2-CDG patients

	Family 1		Family 2	Family 3		Family 4	
Characteristic	**Patient A**	**Patient B**	**Patient C**	**Patient D**	**Patient E**	**Patient F**	**Patient G**
Relation	Siblings		–	Siblings		Siblings	
Sex	Male	Male	Female	Female	Male	Female	Female
Age at last visit	10 years 6 months	6 years 8 months	4 years 4 months	20 years 10 months	13 years 8 months	13 years 5 months	10 years 10 months
Parental descent	Afghan		Italian	Syrian		Egyptian	
Parental consanguinity	First cousins		None known[a]	None known[b]		First cousins once removed	
***GALNT2* genetic changes**							
Amino acid change	p.Gln289*/ p.Gln289*	p.Gln289*/ p.Gln289*	p.Arg200*/ p.Arg200*	p.Tyr99*/ p.Tyr99*	p.Tyr99*/ p.Tyr99*	p.Arg210Pro/ p.Arg210Pro	p.Arg210Pro/ p.Arg210Pro
cDNA change	c.865C>T	c.865C>T	c.598C>T	c.296dup	c.296dup	c.629G>C	c.629G>C
Maternal changes	p.Gln289*/WT		p.Arg200*/WT	p.Tyr99*/WT		p.Arg210Pro/WT	
Paternal changes	p.Gln289*/WT		p.Arg200*/WT	p.Tyr99*/WT		p.Arg210Pro/WT	
ApoC-III western blot							
Non-glycosylated ApoC-III	Yes	Yes	Yes	Yes	Yes	Yes	Yes
Affinity chromatography-MS							
ApoC-III_1/apoC-III_2 ratio	Not performed	Not performed	2.63 (<2.91)	1.35 (<2.91)	1.14 (<2.91)	1.78 (<2.91)	1.45 (<2.91)
ApoC-III_0/apoC-III_2 ratio	Not performed	Not performed	23.87 (<0.48)	13.10 (<0.48)	15.56 (<0.48)	14.48 (<0.48)	19.80 (<0.48)
Transferrin mono-oligo/di-oligo ratio	Not performed	Not performed	0.060 (⩽0.06)	0.070 (⩽0.06)	0.063 (⩽0.06)	0.081 (⩽0.06)	0.049 (⩽0.06)
Transferrin a-oligo/di-oligo ratio	Not performed	Not performed	0.004 (⩽0.011)	0.009 (⩽0.011)	0.004 (⩽0.011)	0.004 (⩽0.011)	0.004 (⩽0.011)
Transferrin tri-sialo/di-oligo ratio	Not performed	Not performed	0.07 (⩽0.05)	0.052 (⩽0.05)	0.038 (⩽0.05)	0.041 (⩽0.05)	0.027 (⩽0.05)

[a]Both grandfathers are from same village (~2000 inhabitants).
[b]Parents are both from the Aleppo area in Syria.
WT = wild-type.

p.Tyr99*) in *GALNT2*. Both parents of the siblings were heterozygous for the *GALNT2* variant, although no consanguinity was reported. The variant was absent from control databases (1000 Genomes, ExAC and gnomAD).

Patients F and G (Family 4) were siblings who were both homozygous for a novel missense variant (c.629G>C; p.Arg210Pro) in *GALNT2*. The consanguineous parents were identified as heterozygous carriers of the variant. The variant was predicted to be disease-causing by MutationTaster and PolyPhen-2 and was absent from control databases (1000 Genomes, ExAC and gnomAD).

ApoC-III isoform analysis results

Based on our previous studies (Schjoldager *et al.*, 2012; Khetarpal *et al.*, 2016), we analysed plasma apoC-III glycosylation by western blot (Fig. 1B and Supplementary Fig. 1) and mass spectrometry to evaluate and confirm loss-of-function of GALNT2. Western blot analysis of healthy control plasma and standard human apoC-III purified from plasma revealed bands of mono- or disialylated apoC-$III_{1/2}$. Plasma from heterozygous parents showed predominant bands of sialylated apoC-$III_{1/2}$, where patient plasma showed only non-glycosylated apoC-III (apoC-III_0), which migrated with a reduced molecular weight of 8–9 kDa.

Mass spectrometry analysis was performed using a clinically available test and demonstrated results consistent with western blot analysis, including significantly increased amounts of the non-glycosylated apoC-III isoform (apoC-III_0) in patient samples (Table 1 and Supplementary Fig. 2). Heterozygous carriers (parents) demonstrated mildly elevated levels of the non-glycosylated apoC-III isoform (apoC-III_0) (Supplementary Table 1 and Supplementary Fig. 3). Unfortunately, available samples of Family 1 were unacceptable for mass spectrometry analysis and parental samples of Family 2 were unavailable.

The clinical utility of apoC-III as a reliable biomarker of GALNT2 loss-of-function was emphasized by the findings of an additional patient with compound heterozygous missense mutations in *GALNT2* but with a dissimilar clinical phenotype (Supplementary material). The western blot analysis demonstrated that this patient had normal levels of sialylated apoC-$III_{1/2}$ (Supplementary Fig. 4), indicating that the variants were likely benign and ruling out a diagnosis of GALNT2-CDG.

Table 2 Clinical characterization, blood test results, brain MRI scans and other paraclinical findings in GALNT2-CDG patients

	Patient A	Patient B	Patient C	Patient D	Patient E	Patient F	Patient G
Growth							
Birth length, m	0.46 (<−2 SD)[a]	0.48 (p15-p25)[a]	0.45 (<−2 SD)[a]	Reportedly normal	Reportedly normal	Reportedly normal	Reportedly normal
Birth weight, kg	2.49 (<−2 SD)[a]	2.86 (p5-p15)[a]	2.3 (<−2 SD)[a]	2.5 (p5)[a]	4.0 (p95)[a]	3.00 (p25–p50)[a]	3.20 (p50)[a]
Head circumference at birth, cm	Not reported	33.0 (p5-p15)[a]	33.0 (p15-p25)[a]	Reportedly normal	Reportedly normal	Reportedly normal	Reportedly normal
Age at last measurement	9 y 0 mo	6 y 3 mo	4 y 4 mo	20 y 10 mo	13 y 8 mo	13 y 5 mo	10 y 10 mo
Height at last measurement, m	1.27 (p15–p25)[a]	1.16 (p15–p25)[a]	0.98 (p5–p15)[a]	1.45 (<−2 SD)[a]	1.45 (<−2 SD)[a]	1.48 (p5–p15)[a]	1.29 (<−2 SD)[a]
Weight at last measurement, kg	27.0 (p25–p50)[a]	20.0 (p15–p25)[a]	14.1 (p5–p15)[a]	45.5 (p3–p10)[b]	43.5 (p10–p25)[b]	57.0 (p75–p90)[b]	45.0 (p75–p90)[b]
Head circumference at last measurement, cm	51.5 (p10–p25)[c]	51.5 (p25–p50)[c]	47.0 (p3–p5)[a] (<p3)[c]	51.1 (<p3)[c]	52.0 (p3–p10)[c]	55.5 (p90–p97)[c]	54.0 (p75–p90)[c]
Microcephaly	No	No	Yes	Yes	No	No	No
Psychomotor development							
Gross motor delay	Severe	Severe	Moderate	Moderate	Moderate	No	No
Sitting age; age of independent walking	12 mo; 6 y	18 mo; 6 y	21 mo; 3 y	8 mo; 2 y	8 mo; 2 y	7 mo; 13 mo	7 mo; 15 mo
Intellectual disability	Severe	Severe	Severe	Moderate–severe	Severe	Moderate	Severe
Understands commands	Few commands	Few commands	Almost absent	Good understanding	Few commands	Good understanding	Several commands
Expressive speech	Few words	Absent	Absent	Absent	Absent	Few words	Absent
Loss of psychomotor function	No	No	No	No	Yes; loss of words	Yes; loss of words	Yes; loss of words
Neurological							
Eye contact	Poor	Poor	Poor	Good	Poor	Average	Poor
Autistic behaviour	Yes	Yes	Yes	No	Yes	Yes	Yes
Behavioural problems	Yes	Yes	Yes	No	No	Yes	Yes
Epilepsy; age of onset	Yes; 2.5 y	Yes; 2.5 y	Yes; 4 mo	Yes; 1 year	Yes; 1.5 y	No	Yes; 4 y
Type of epilepsy, EEG	Multifocal	Multifocal	Infantile spasms	Multifocal, eye-closure sensitivity	Multifocal, eye-closure sensitivity	N/A	Head drops
Current epilepsy status	Seizure-free on meds	Treatment-resistant	Seizure-free on meds	Treatment-resistant	Treatment-resistant	N/A	Restarted on medication
Sleeping problems	Chronic insomnia	Chronic insomnia	Chronic insomnia	No	Chronic insomnia	Chronic insomnia	Chronic insomnia
Vision, eye examination	Alternating strabismus	Normal	Myopic astigmatism	Normal	Normal	Mild nystagmus	Normal
Hearing	Perceived as normal	Perceived as normal	Bilateral conductive hearing loss	Perceived as normal	Perceived as normal	Normal	Normal
Blood tests							
Total cholesterol, mg/dl	124[d]	ND	148 (120–200)	85 (<193)	124 (<193)	161 (70–200)	139 (70–200)
HDL-cholesterol, mg/dl	27[d]	ND	34 (>30)	43 (>39)	25 (>39)	41 (35–65)	38 (35–65)
LDL-cholesterol, mg/dl	51[d]	ND	98 (50–150)	31 (<116)	81 (<116)	108 (70–135)	76 (70–135)
Triglyceride, mg/dl	93[d]	ND	99 (40–150)	68 (<177)	76 (<177)	57 (35–135)	124 (35–135)
Creatinine, mg/dl	0.28 (0.53–0.79)	0.31 (0.40–0.60)	0.23 (0.20–0.90)	0.41 (0.57–1.02)	0.53 (0.59–1.05)	0.49 (0.5–1.1)	0.42 (0.5–1.0)
Findings	WML, brachycephaly	WML, brachycephaly	WML; regional myelination arrest; small pineal cyst; microcephaly	WML; mild cerebellar atrophy; thickened calvarium; microcephaly	WML	Discrete WML; persisting cavum septum pellucidum with cavum vergae	No WML; small pineal cyst

GGT = gamma-glutamyltransferase; IDA = iron deficiency anaemia; NA = not applicable; ND = not determined; p = percentile; WML = white matter lesions. See Supplementary Table 2 for a full version of this table.
Growth charts: [a]WHO growth charts; [b]Centers for Disease Control and Prevention (CDC) Growth Charts; [c]Rollins *et al.* (2010). United States Head Circumference Growth Reference Charts: Birth to 21 Years.
[d]Reported by Khetarpal *et al.* (2016).
[e]For blood test results, 'Normal' refers to results within the reference interval of the parameter.
[f]Corrected with iron supplementation.

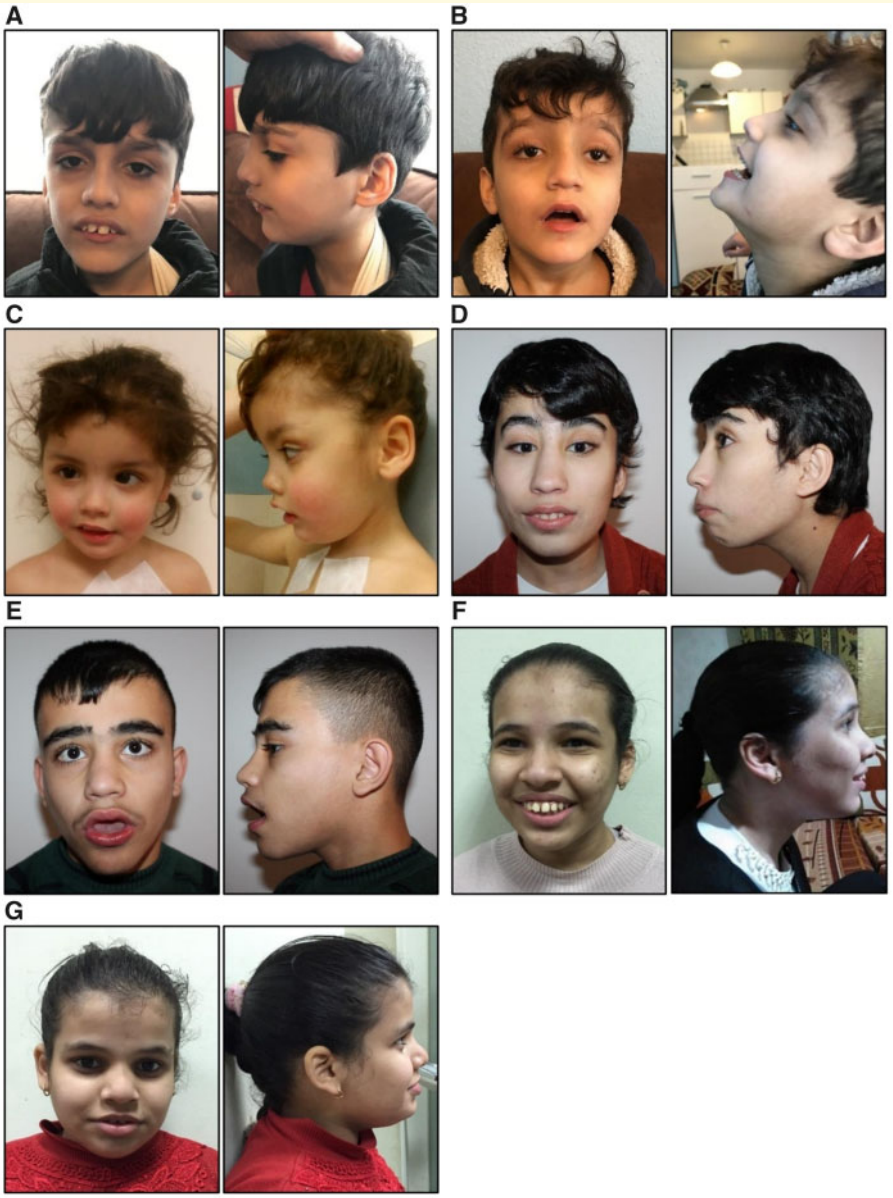

Figure 2 Front and side photographs of patients diagnosed with GALNT2-CDG. GALNT2-CDG patients shared dysmorphic facial features including elongated face, high forehead, almond-shaped eyes, protruding maxilla, short philtrum, low-set, posteriorly rotated ears and frequently full lips with a tented or curved upper lip. (**A**) Patient A additionally had down-slanting palpebral fissures, macrodontia, wide-spaced teeth, and broad chin. (**B**) Patient B shared down-slanting palpebral fissures with his brother (Patient A) and additionally had sparse medial and curved eyebrows, dense eyelashes, and hypertelorism. (**C**) Patient C additionally had sparse lateral eyebrows, hypertelorism, midface hypoplasia, depressed nasal bridge, anteverted nares, and downturned corners of the mouth. (**D**) Patient D additionally had arched eyebrows, dense eyelashes laterally, and high nasal bridge. (**E**) Patient E additionally had bushy eyebrows, dense eyelashes, and high nasal bridge. He also had pointed canines in upper jaw (not shown). (**F**) Patient F additionally had a broad nose, macrostomia, macrodontia, wide-spaced teeth, and a broad chin. (**G**) Patient G additionally had sparse lateral eyebrows, broad nose, hypoplastic nasal alae, macrostomia, macrodontia, wide-spaced teeth, and ears with fleshy lobules.

Clinical characteristics

Patient clinical characteristics are summarized in Table 2 and Supplementary Table 2. For details of individual patients, see the Supplementary material. For patient photographs and dysmorphic facial features, see Fig. 2.

Growth

All patient heights were <25th percentile, and three patients had short stature (<–2 SD). In Patient E, bone age was found to be the same as chronological age. Two patients had microcephaly.

Dysmorphic facial features

All patients exhibited some degree of dysmorphic facial features (Fig. 2), commonly including elongated face, high forehead, almond-shaped eyes, protruding maxilla, short philtrum, low-set, posteriorly rotated ears and frequently full lips with a tented or curved upper lip.

Psychomotor developmental delay and autistic features

All seven patients demonstrated delays in psychomotor development. Five of seven patients were delayed in gross motor function with age for independent walking between 2 years and 6 years. Patients F and G walked independently at age 13 months and 15 months, respectively. All patients had varying degrees of language deficits with the ability to understand commands extending from good (Patients D and F) to almost absent. Expressive speech was absent for five patients, while two patients were capable of saying a few words (Patients A and F).

Formal testing for autism spectrum disorder was not performed; however, six patients displayed autistic behaviours (i.e. lack of interest in others, delayed language development and stereotypical movements and behaviour). Three patients had loss of a few words at 2 years of age, but loss of psychomotor function was otherwise not seen in this patient group.

Epilepsy

Six patients had epilepsy of varying types and severities. The remaining patient (Patient F) was treated for suspected epilepsy after a febrile seizure at age 1 year, but the diagnosis was later dismissed (Supplementary material). Patient C had infantile spasms starting at 4 months of age and was seizure-free with treatment by 12 months. Four patients had onset of multifocal epilepsy with various seizure types beginning at 1–2.5 years. In three of these patients, epilepsy was treatment-resistant. One patient (Patient G) had epileptic drop attacks of the head beginning at 4 years that were successfully treated with ethosuximide.

Sleep disturbances

Sleep disturbance was a prominent feature in this patient group. Six patients had chronic insomnia with problems falling asleep, sleep disruption and daytime tiredness or sleepiness at least three times a week for the last 3 months (Pradeep *et al.*, 2019). In all of the six patients the chronic insomnia was of years duration. Melatonin therapy improved the insomnia in four patients, and had no effect in two patients (Supplementary material). Sleep study showed parasomnias in one patient (Patient B). In Patient E, disrupted sleep was partly due to night-time seizures documented during long-term video-EEG monitoring, but awakenings were also seen, when no seizures were registered (EEG results not shown).

Brain MRI findings

Brain MRI scans were obtained using various protocols for all seven patients at various ages (Fig. 3). For detailed descriptions of brain MRI scans, see the Supplementary material. White matter lesions were observed on scans of six of the seven patients (Table 2 and Supplementary Table 2), but varied in their patterns and locations among patients.

Laboratory findings

Blood test results are summarized in Table 2 and Supplementary Table 2 with reference intervals as stated by the performing local laboratory. Patient A was previously reported to have a fasting lipid profile with HDL-C level below the fifth percentile and a moderately low triglyceride level (Khetarpal *et al.*, 2016). Lower HDL-C levels were seen in five other patients; Patient E had HDL-C level below the reference interval, and four patients had HDL-C levels just above the lower level of the reference interval. The lipid profile for Patient B was not examined. Fasting triglyceride levels ranged from low (Patients D–F) to high in the reference interval (Patient G). Four patients had iron-deficiency anaemia with low haemoglobin and ferritin levels corrected with iron supplementation. White blood cell counts and platelet counts as well as bilirubin and thyroid parameters were normal in all patients. Six patients had low vitamin D levels corrected with vitamin D supplementation. The patients showed decreased levels of serum creatinine.

GALNT2-CDG rodent models

Physical parameters

Given the multisystem involvement of GALNT2-CDG patients, we pursued further characterization of germline *Galnt2* knockout rodent models of GALNT2-CDG (Khetarpal *et al.*, 2016). Significant embryonic lethality occurred in both rodent knockout models (Supplementary material). In surviving animals we observed decreased body weight in male knockout mice [$F(2,66) = 11.27$, $P = 6.2 \times 10^{-5}$; Fig. 4B], female knockout rats [$F(2,20) = 4.60$, $P = 0.02$; Fig. 4C] and male knockout rats [$F(2,21) = 11.91$, $P = 0.0003$; Fig. 4D]. We also observed mildly increased liver weights in knockout mice (Supplementary Fig. 5A). Additionally, knockout rodents had abnormal craniofacial features with decreased snout length (Fig. 4E and F).

Behavioural phenotypes

Analysis of spontaneous open field activity showed increased centre [$t(1,25) = 3.21$, $P = 0.004$; Supplementary Fig. 6B] and rearing activities [$t(1,25) = 3.394$, $P = 0.002$; Supplementary Fig. 6C] of *Galnt2* knockout compared to wild-type littermates with normal horizontal activity [$t(1,25) = 0.43$, $P = 0.67$; Supplementary Fig. 6A]. On accelerating rotarod testing, knockout mice showed reduced latency to fall [$F(1,28) = 11.06$, $P = 0.002$; Fig. 5A]. On acoustic startle response and prepulse inhibition testing, knockout mice

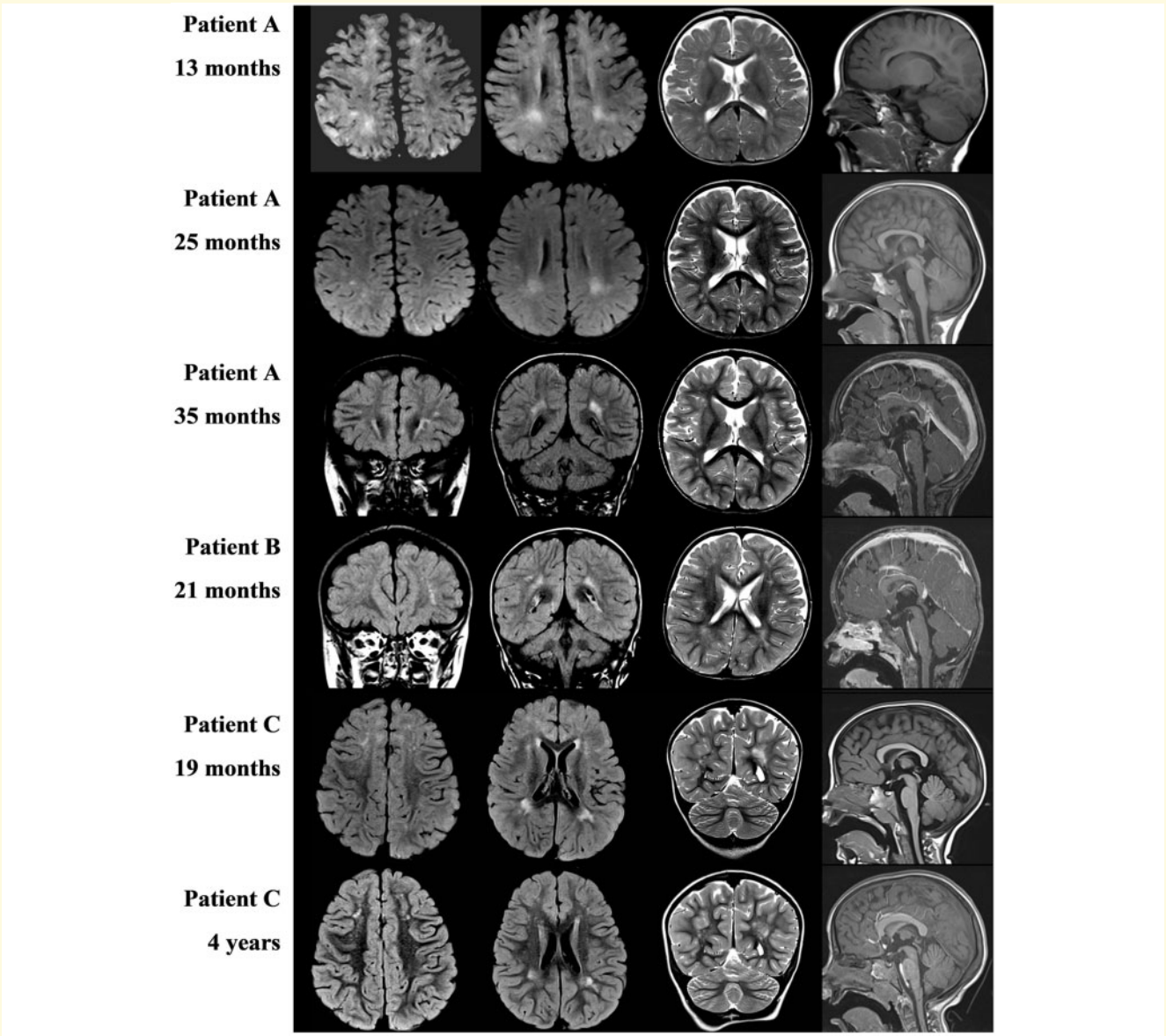

Figure 3 Brain MRI results obtained from seven GALNT2-CDG patients at different ages. MRI scans showed white matter lesions in scans from Patients A–F but not in scan from Patient G. Patient age at the time of the MRI scan is shown. Columns 1 and 2 depict axial FLAIR images (or coronal FLAIR for Patient A at 35 months, Patient B, and Patient F). Column 3 depicts T_2-weighted images in axial view (or coronal view for Patients C–E). Column 4 depicts sagittal T_1-weighted images (with intravenous contrast for Patient A at 35 months and Patient B).

showed potentiated habituation to acoustic stimuli [$t(1,27) = 2.18$, $P = 0.04$; Fig. 5B] and disrupted prepulse inhibition [$t(1,27) = 2.02$, $P = 0.05$; Fig. 5C] with similar responses to increases in acoustic stimulus intensities [$F(1,27) = 1.95$, $P = 0.17$; Supplementary Fig. 6D]. On social preference testing, *Galnt2* knockout mice showing reduced exploration of the social cue [$F(1,44) = 7.87$, $P = 0.007$; Fig. 5D], with intact olfaction [$F(3,46) = 9.85$, $P = 3.9 \times 10^{-5}$; Supplementary Fig. 7], the primary sensory mediator of murine social behaviour.

Discussion

Here, we describe seven patients with a novel autosomal recessive congenital disorder of O-glycosylation, GALNT2-CDG, and validate plasma apoC-III as a biomarker of the disease. Clinically GALNT2-CDG patients demonstrated global developmental delay, intellectual disability with language deficit, autistic features, behavioural abnormalities, epilepsy, chronic insomnia, decreased stature, and white matter lesions on brain MRI scan. GALNT2-CDG patients

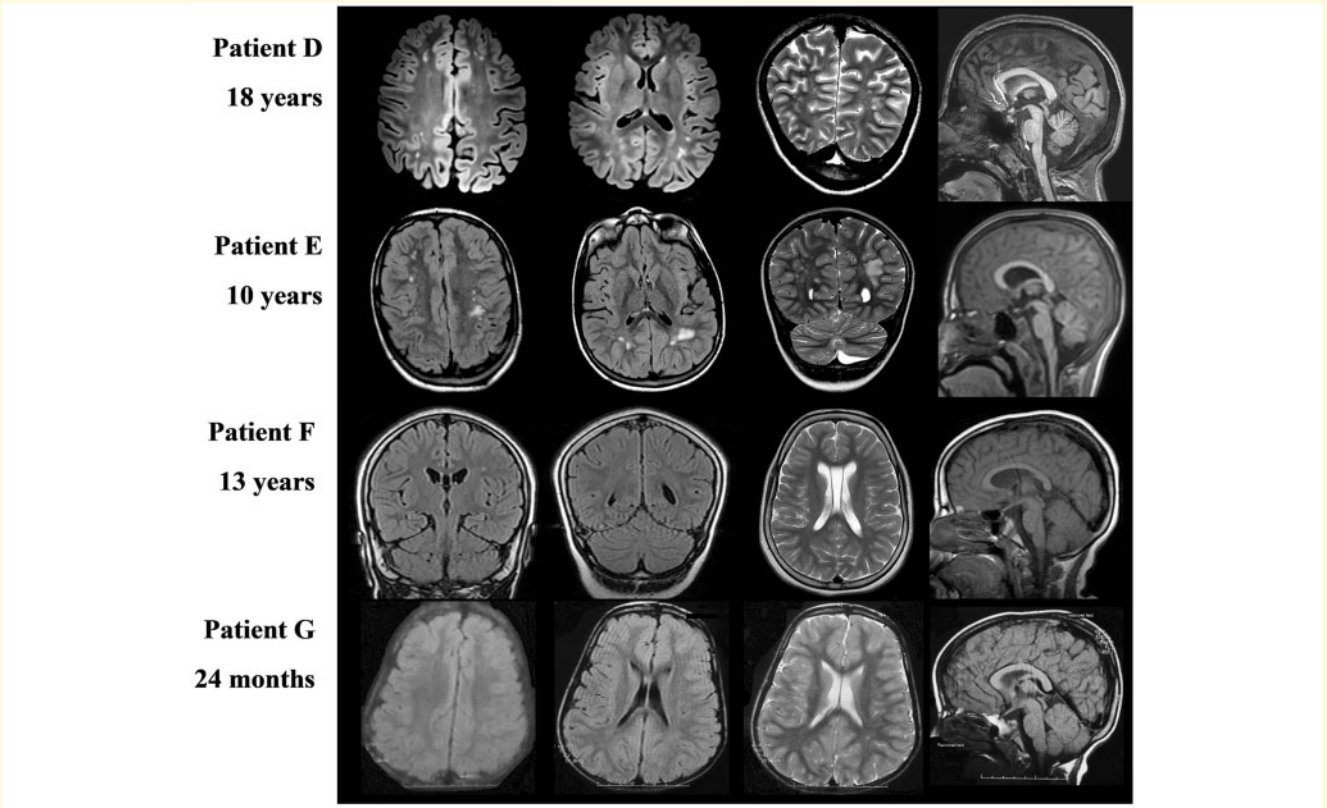

Figure 3 Continued

also had some dysmorphic facial features in common though not comprising a recognizable dysmorphic facial phenotype.

Because of their clinical variability, directly diagnosing GALNT2-CDG in patients with developmental delay is challenging. In patients with developmental delay, the presence of dysmorphic features, epilepsy appearing in the first years of life, and brain MRI abnormalities make a genetic aetiology likely. In such patients, coinciding decreased growth or short stature, white matter lesions on brain MRI, and decreased HDL-C would particularly suggest consideration of GALNT2-CDG. Hence, clinical work-up suggested would be a comprehensive history including family history and consanguinity, physical examination, growth chart evaluation, blood chemistry including fasting lipid levels, EEG, brain MRI scan, evaluation of vision and hearing, and genetic testing with WES.

Validating pathogenic variants in glycosyltransferase genes, such as *GALNT2*, is difficult. Prediction algorithms perform poorly for these genes (Hansen *et al.*, 2015), and labour-intensive experimental assays may be prone to uncertainties (Guda *et al.*, 2009). To aid in interpretation of *GALNT2* variants identified in NGS or WES studies, we validated complete loss of *O*-glycans on the abundant plasma apoC-III *O*-glycoprotein as a diagnostic assay of GALNT2-CDG. Highlighting the clinical utility of the assay, an eighth patient with a dissimilar clinical presentation and compound heterozygous variants in *GALNT2* had normal apoC-III glycosylation, which ruled out GALNT2 deficiency.

GALNT2 polymorphisms were first associated with plasma lipids in GWAS (Kathiresan *et al.*, 2008), and GALNT2 loss-of-function was later confirmed to decrease HDL-C levels in rodent knockout models (Khetarpal *et al.*, 2016). All patients with available fasting lipid profiles had lower plasma HDL-C levels, consistent with previous findings (Khetarpal *et al.*, 2016).

Rodent *Galnt2* knockout models recapitulated clinical features of GALNT2-CDG patients, including growth differences, abnormal craniofacial morphology, and neurobehavioural anomalies. The observed deficits in coordination, sensory-motor integration, and sociability suggest that multiple neurological pathways are altered in *Galnt2*-deficient models, potentially including dopamine-dependent (Karasinska *et al.*, 2000), GABAergic (Liu *et al.*, 2007) and serotoninergic (Kelley *et al.*, 2003) pathways. Our rodents are limited as models of GALNT2-CDG because of significant embryonic lethality and the clinical heterogeneity of GALNT2-CDG patients. However, shared neurodevelopmental abnormalities suggest that important insights will come from further studies of the roles of GALNT2 in the developing brain.

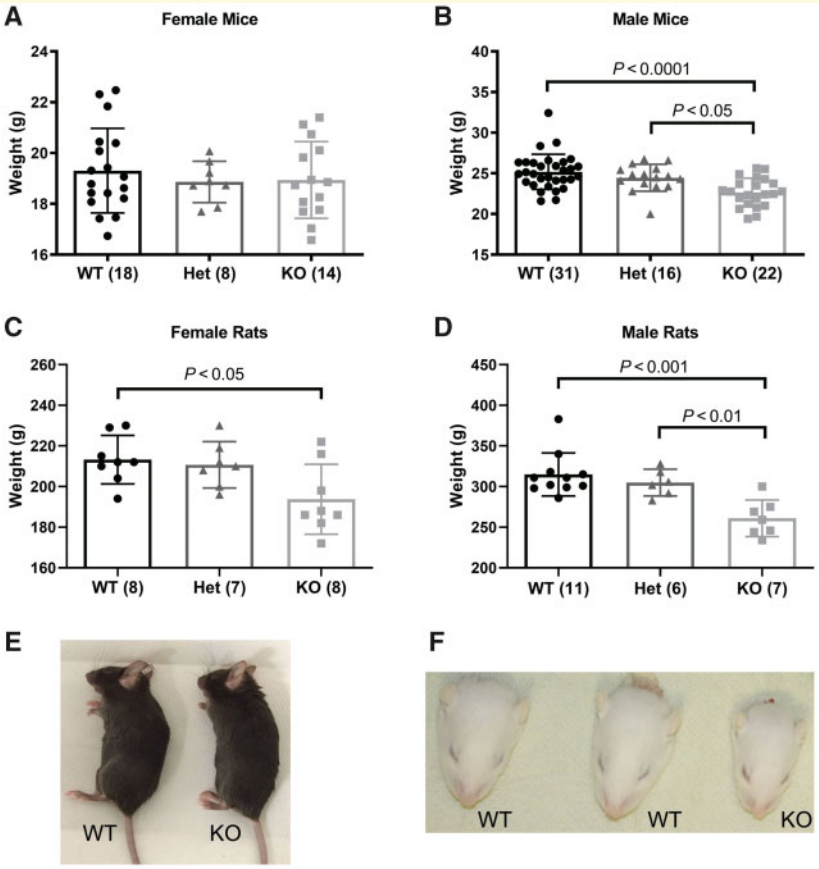

Figure 4 Growth parameters of GALNT2-CDG rodent models. Bar plots of the mean body weight of wild-type (WT), *Galnt2*$^{+/-}$ heterozygous (Het), and *Galnt2*$^{-/-}$ (KO) rodents are shown for (**A**) female mice, (**B**) male mice, (**C**) female rats, and (**D**) male rats. Representative pictures of wild-type and knockout (**E**) mice and (**F**) rats are shown. Error bars represent standard deviation. Significant *P*-values from Tukey's post-test are indicated. Number of animals is indicated in parenthesis.

The high prevalence of neurological disease among CDG patients highlights the brain's dependence on various glycosylation types. Deficiencies in several glycosylation pathways, including GalNAc-type *O*-glycosylation, can cause epilepsy ranging in severity from easily controlled to severe epileptic encephalopathy (Morava *et al.*, 2012; Arranz *et al.*, 2014). Glycosylation deficiency can also result in brain MRI white matter lesion changes as seen in GALNT2-CDG, which were non-specific and without a shared neuroimaging pattern. Non-specific white matter lesions have been reported in other CDG types, such as dystroglycanopathies and SLC35A2-CDG. These CDGs involve distinct glycosylation types from the GalNAc-type glycosylation in GALNT2-CDG. Dystroglycanopathies result from mutations in glycosyltransferase enzyme genes involved in *O*-mannosylation (Clement *et al.*, 2008) and SLC35A2-CDG is a disorder of *N*-linked glycosylation (Vals *et al.*, 2019).

GALNT2-CDG patients suffer from multisystemic disease manifestations, suggesting non-redundant functions of GALNT2 beyond the previously identified specific glycosylation of proteins involved in lipid metabolism, including ANGPTL3, apoC-III and PLTP. Deficient *O*-glycosylation of PLTP reduces phospholipid transfer to HDL and lowers HDL-C levels (Khetarpal *et al.*, 2016); however, PLTP is broadly expressed throughout the body, including by neurons and glial cells in the brain (Vuletic *et al.*, 2003) potentially influencing neuro-pathogenesis in GALNT2-CDG patients. GALNT2 is ubiquitously expressed in all mammalian cells and tissues and the function of GALNT2 will depend on the available substrates and repertoire of other GALNT isoenzymes expressed in a given cell. In most cells and tissues analysed so far, GALNT2 has only a minor non-redundant, isoform-specific contribution to the *O*-glycoproteome (Schjoldager *et al.*, 2015; Khetarpal *et al.*, 2016). Thus, the GALNT2-CDG disease pathophysiology likely involves deficient GALNT2 *O*-glycosylation on a subset of target glycoproteins. Additional studies to identify the protein substrates of GALNT2 will reveal important insights into the pathophysiology and phenotypes of GALNT2-CDG, as well as the critical role of *O*-glycosylation in the normal function of substrate proteins, particularly in neurodevelopmental biology.

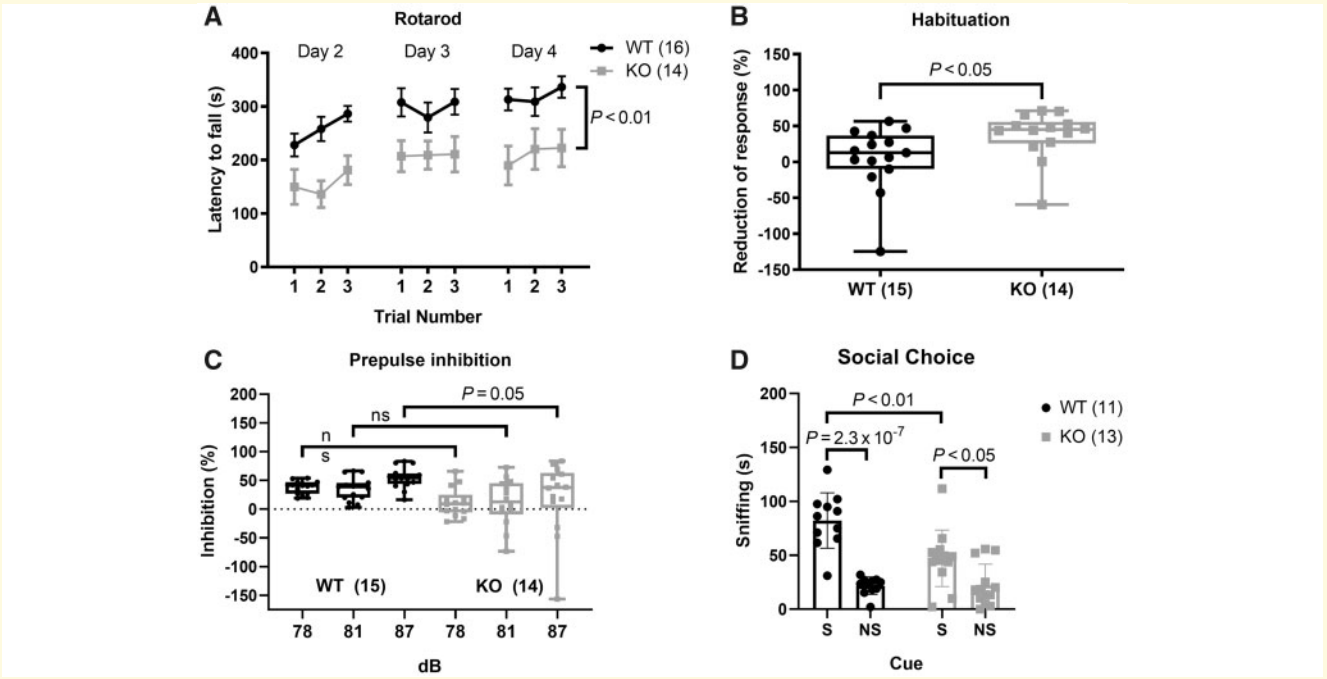

Figure 5 Behavioural analysis of GALNT2-CDG mouse model. (**A**) Results of accelerating rotarod testing of coordination in wild-type (WT) and *Galnt2* knockout (KO) mice. Data represented as mean values and error bars represent standard error of the mean (SEM). (**B**) Startle response was measured by displacement of a fixed platform in response to auditory stimulus (Supplemental material). Habituation was measured by comparing displacement from the first five 120 dB stimuli to the last five 120 dB stimuli. (**C**) Disruption of the normal startle response by initial smaller auditory prepulse stimuli of increasing intensities from 78 to 87 dB, followed by startle-evoking 120 dB stimulus. Data represented in box and whisker plots of mean values. Whiskers represent maximum and minimum values. (**D**) Time spent sniffing the area around a social cue (S, another mouse) or non-social inanimate cue (NS). Data represented with box plots of mean values. Error bars represent standard deviation. Significant *P*-values from (**A**) repeated measures ANOVA, (**B** and **C**) Student's unpaired *t*-test, (**D**) Tukey's post-test, or indicated as non-significant (ns). Number of mice indicated in parenthesis.

Acknowledgements

We would like to thank the families for their participation in this study. We thank the Broad Institute (HG008900 to Daniel MacArthur and Heidi Rehm). Mouse behavioural phenotyping was performed at the Neurobehavior Testing Core at the University of Pennsylvania/ITMAT and IDDRC at the Children's Hospital of Philadelphia/Penn U54 HD086984. We thank Dr Zhaolan Zhou for his helpful guidance with the manuscript and Dr Kathryn Kadash for her critical review of the manuscript.

Funding

This work was supported by the Foundation Leducq CVGeneF(x) Transatlantic Network of Excellence grant to D.J.R., supported by the Magnus Ehrnrooth Foundation to U.P.R., by National Institutes of Health grants F30HL124967 to S.A.K., T32 GM008638 to A.C.E., and U54 NS115198 to A.C.E. and K.R., and by the Danish National Research Foundation (DNRF107) and a Novo Nordisk Foundation Excellence grant to K.S.

Competing interests

The authors report no competing interests.

Supplementary material

Supplementary material is available at *Brain* online.

References

Abou Jamra R, Wohlfart S, Zweier M, Uebe S, Priebe L, Ekici A, et al. Homozygosity mapping in 64 Syrian consanguineous families with non-specific intellectual disability reveals 11 novel loci and high heterogeneity. Eur J Hum Genet 2011; 19: 1161–6.

Arranz AM, Perkins KL, Irie F, Lewis DP, Hrabe J, Xiao F, et al. Hyaluronan deficiency due to Has3 knock-out causes altered neuronal activity and seizures via reduction in brain extra extracellular space. J Neurosci 2014; 34: 6164–76.

Ashwal S, Michelson D, Plawner L, Dobyns WB, Practice parameter: evaluation of the child with microcephaly (an evidence-based review). Neurology 2009; 73: 887–97.

Clement E, Mercuri E, Godfrey C, Smith J, Robb S, Kinali M, et al. Brain involvement in muscular dystrophies with defective dystroglycan glycosylation. Ann Neurol 2008; 64: 573–82.

Guda K, Moinova H, He J, Jamison O, Ravi L, Natale L, et al. Inactivating germ-line and somatic mutations in polypeptide N-acetylgalactosaminyltransferase 12 in human colon cancers. Proc Natl Acad Sci U S A 2009; 106: 12921–5.

Hansen L, Lind-Thomsen A, Joshi HJ, Pedersen NB, Have CT, Kong Y, et al. A glycogene mutation map for discovery of diseases of glycosylation. Glycobiology 2015; 25: 211–24.

Jaeken J, Peanne R, What is new in CDG? J Inherit Metab Dis 2017; 40: 569–86.

Joshi HJ, Hansen L, Narimatsu Y, Freeze HH, Henrissat B, Bennett E, et al. Glycosyltransferase genes that cause monogenic congenital disorders of glycosylation are distinct from glycosyltransferase genes associated with complex diseases. Glycobiology 2018; 28: 284–94.

Karasinska JM, George SR, El-Ghundi M, Fletcher PJ, O'Dowd BF, Modification of dopamine D_1 receptor knockout phenotype in mice lacking both dopamine D_1 and D_3 receptors. Eur J Pharmacol 2000; 399: 171–81.

Kathiresan S, Melander O, Guiducci C, Surti A, Burtt NP, Rieder MJ, et al. Six new loci associated with blood low-density lipoprotein cholesterol, high-density lipoprotein cholesterol or triglycerides in humans. Nat Genet 2008; 40: 189–97.

Kato K, Jeanneau C, Tarp MA, Benet-Pagès A, Lorenz-Depiereux B, Bennett EP, et al. Polypeptide GalNAc-transferase T3 and familial tumoral calcinosis. Secretion of fibroblast growth factor 23 requires O-glycosylation. J Biol Chem 2006; 281: 18370–7.

Kelley SP, Bratt AM, Hodge CW, Targeted gene deletion of the 5-HT3A receptor subunit produces an anxiolytic phenotype in mice. Eur J Pharmacol 2003; 461: 19–25.

Khetarpal SA, Schjoldager KT, Christoffersen C, Raghavan A, Edmondson AC, Reutter HM, et al. Loss of function of GALNT2 lowers high-density lipoproteins in humans, nonhuman primates, and rodents. Cell Metab 2016; 24: 234–45.

Liu GX, Cai GQ, Cai YQ, Sheng ZJ, Jiang J, Mei Z, et al. Reduced anxiety and depression-like behaviors in mice lacking GABA transporter subtype 1. Neuropsychopharmacology 2007; 32: 1531–9.

Morava E, Vodopiutz J, Lefeber DJ, Janecke AR, Schmidt WM, Lechner S, et al. Defining the phenotype in congenital disorder of glycosylation due to ALG1 mutations. Pediatrics 2012; 130: e1034–9.

Ng BG, Freeze HH, Perspectives on glycosylation and its congenital disorders. Trends Genet 2018; 34: 466–76.

Pradeep C, Bollu MD, Kaur H. Sleep medicine: insomnia and Sleep. Mo Med 2019; 116: 68–75.

Quigley CA, Ranke MB. International classification of pediatric endocrine diagnoses 2016. www.icped.org.

Reuter MS, Tawamie H, Buchert R, Hosny Gebril O, Froukh T, Thiel C, et al. Diagnostic yield and novel candidate genes by exome sequencing in 152 consanguineous families with neurodevelopmental disorders. JAMA Psychiatry 2017; 74: 293–9.

Rollins JD, Collins JS, Holden KR, United States head circumference growth reference charts: birth to 21 years. J Pediatr 2010; 156: 907–13.

Schjoldager KT, Joshi HJ, Kong Y, Goth CK, King SL, Wandall HH, et al. Deconstruction of O-glycosylation-GalNAc-T isoforms direct distinct subsets of the O-glycoproteome. EMBO Rep 2015; 16: 1713–22.

Schjoldager KT, Vakhrushev SY, Kong Y, Steentoft C, Nudelman AS, Pedersen NB, et al. Probing isoform-specific functions of polypeptide GalNAc-transferases using zinc finger nuclease glycoengineered SimpleCells. Proc Natl Acad Sci U S A 2012; 109: 9893–8.

Sobreira N, Schiettecatte F, Valle D, Hamosh A, GeneMatcher: a matching tool for connecting investigators with an interest in the same gene. Hum Mutat 2015; 36: 928–30.

Topaz O, Shurman DL, Bergman R, Indelman M, Ratajczak P, Mizrachi M, et al. Mutations in GALNT3, encoding a protein involved in O-linked glycosylation, cause familial tumoral calcinosis. Nat Genet 2004; 36: 579–81.

Vals MA, Ashikov A, Ilves P, Loorits D, Zeng Q, Barone R, et al. Clinical, neuroradiological, and biochemical features of SLC35A2-CDG patients. J Inherit Metab Dis 2019; 42: 553–64.

Vuletic S, Jin LW, Marcovina SM, Peskind ER, Moller T, Albers JJ, Widespread distribution of PLTP in human CNS: evidence for PLTP synthesis by glia and neurons, and increased levels in Alzheimer's disease. J Lipid Res 2003; 44: 1113–23.

Wit JM, Ranke MB and Kelnar CJH. ESPE classification of paediatric endocrine diagnosis. 1. Short stature. Horm Res 2007; 68: 1–5.

Wopereis S, Grunewald S, Huijben KM, Morava E, Mollicone R, van Engelen BG, et al. Transferrin and apolipoprotein C-III isofocusing are complementary in the diagnosis of N- and O-glycan biosynthesis defects. Clin Chem 2007; 53: 180–7.